IIETA International Information and Engineering Technology Association
Advancing the World of Information and Engineering

Mathematical Modelling of Engineering Problems
Vol. 11, No. 5, May, 2024, pp. 1189-1197
Journal homepage: http://iieta.org/journals/mmep

Effect of 3D Printing Parameters on Hollow Vascular Networks for Self-Healing Concrete Using Recycled Materials

Noor A. Hameed*, Farhad M. Othman, Alaa A. Abdul-Hamead

Department Materials Engineering, University of Technology, Baghdad 19006, Iraq

Corresponding Author Email: Mae.20.101@grad.uotechnology.edu.iq

https://doi.org/10.18280/mmep.110507

Received: 23 September 2023
Revised: 28 November 2023
Accepted: 12 December 2023
Available online: 30 May 2024

Keywords:
hollow pipes, fused deposition modelling, layer thickness, mechanical properties, self-healing concrete, recycling, poly lactic acid

ABSTRACT

Self-healing concrete can repair and seal cracks, this study explores fused deposition modelling (FDM) for creating novel vascular networks and tubes using polylactic acid (PLA) as a material they are incorporated within the concrete beam to injection the healing agent. The problem addressed in the text is to understand how interaction different printing parameters on different layer thicknesses (0.10, 0.20, 0.30, 0.40, and 0.50) mm affect the mechanical properties of (PLA) samples produced through (FDM) with a 3D printer, which was investigated using standardized tests. The hardness and tensile strength were determined using the ASTM D2240 method and ASTM D638-10, while water absorption was assessed using the ISO 62 standard. The bending properties of the specimens were analyzed using the ASTM D790-10 three-point bending test. Tensile and flexural strength increased up to 72 MPa and 81 MPa respectively as layer thickness increased up to 0.4 this layer was chosen to print the hollow vascular network.

1. INTRODUCTION

Building objects with lightweight and complicated structures in 3D is specified as a process referred to as additive manufacturing (AM) which is commonly known as the 3D printing. The use of such technology has increased significantly over the past ten years and is widespread in various industries, such as building, engineering, aerospace, medicine, etc. [1]. Fused deposition modeling (FDM) can be defined as one of the additive manufacturing building techniques which add thermoplastic materials layer by layer using an extrusion nozzle, like polyethylene terephthalate glycol (PETG), acrylonitrile butadiene styrene (ABS), polylactic acid (PLA), and polycarbonate (PC). Also, it represents the most popular approach that is utilized in the additive manufacturing since it's easy to employ, affordable, utilizes multiple materials, and processes parts quickly compared to conventional manufacturing [2]. Due to its environmental friendliness, low cost, biodegradability, and good adaptability to various materials, such as carbon, nylon, and a few other fibers, PLA is the most widely utilized material in FDM. [3]. Throughout a long period of time, numerous investigations on the impact of printing layer thickness on the mechanical characteristics and using recycled materials in Cementous material materials have been carried out, including the following: Chacón et al. [4] studied the impact of feed rate and layer thickness on PLA samples' mechanical properties using a 3D printer. They conducted tensile and 3-point bending tests, observing anisotropic behavior and a decrease in ductility with increasing feed rate and layer thickness. The mechanical properties showed an upward trend with layer thickness, while on-edge and flat orientations showed little significance.

Liu et al. [5] studied the impact, tensile, and flexural strength of PLA parts using fused deposition modeling (FDM). Factors considered included deposition orientation, style, gap, width, and layer thickness. The study used the Taguchi system and ANOVA to evaluate parameters' impact on component quality. Grey relational analysis was used to develop optimal process parameter combinations. Aveen et al. [6] Investigated the use of desktop 3D printing for fabricating technical components utilizing PLA and bronze loaded PLA. The mechanical characteristics of these materials were evaluated, revealing that PLA exhibited superior tensile and flexural strength in comparison to bronze filled PLA. The results indicate that using PLA in 3D printing shows promise for engineering purposes.

Vinyas et al. [7] examined the impact of carbon fibers and nylon glass fibers on the mechanical characteristics of PLA composites produced through Fused Deposition Modelling. The findings indicate that PLA + PETG emerges as a favorable option owing to its exceptional mechanical characteristics, rendering it well-suited for the production of biodegradable consumer goods.

Ayrilmis et al. [8] examined the impact of the thickness of printing layer upon the technological characteristics of the 3D-printed specimens made from wood flour/PLA filaments with a diameter of (1.75 mm). The 3D-printed samples' water absorption increased as the printing layer thickness rose from (0.05 mm) to (0.3 mm). And, this could be clarified through the truth that as the layer thickness grew, there was more empty space in 3D-printed sample, which caused it to absorb more water. With a reduction in the thickness of printing layer, the bending and tensile capabilities of wood/PLA composite

specimens produced in 3D dramatically enhanced.

Behnam and Mojtaba [9] researched composite sample parts made of ABS granules as a polymeric matrix and Cu particles with fixed 25wt% of the metallic powder as filler. The best operating parameters of a filament manufacture line used for acquiring printable filaments were reported. For an examination into the tensile strength, density, and time of manufacture of composite samples, three levels of 4 printing parameters, which include—raster angle, nozzle diameter, layer height, and nozzle temperature—were selected.

Ali et al. [10] indicated that the most important variables affecting how specimen tensile and compressive behavior affects Acrylonitrile-Butadiene-Styrene (ABS) components made with the use of FDM are infill density, infill pattern, and layer thickness as the density increased from 20% to 60%, the material's tensile and compressive properties get better.

Triyono et al. [11] studied the nozzle diameter impact upon the ultimate tensile stress (UTS) of 3D-printed polylactic acid (PLA) items. The research's nozzle sizes ranged from 0.3 to 0.6 mm. 20% of nozzle diameter was chosen as layer thickness. It was discovered that the UTS also grows when the nozzle diameter does. It was discovered using SEM imaging that the decrease in voids (air gaps) between adjusting strands was what caused the increase in UTS. The findings of the study indicated that the augmentation of nozzle hole diameters resulted in an increase in both density and tensile strength The raster becomes broader as the nozzle diameter is raised, and adjacent strands overlap and fuse together throughout the solidification process.

Bakir et al. [12] proposed fused deposition modeling (FDM) filaments made from recycled materials are ideal for eco-conscious and sustainable production of prototypes and load-bearing components such PET. Research shows that increasing nozzle temperature by 260°C doubles specimen strength, while aligning raster orientation parallel to loading direction increases ductility by ten. The Gibson-Ashby model predicts strength and infill ratio, making FDM a viable manufacturing technique for load-bearing applications.

Ming-Hsien Hsueh, et al. [13] improved fused deposition modeling (FDM) efficiency by examining the impact of printing and raster angles on tensile properties of polylactic acid (PLA) specimens. UV curing was also examined, finding that printing and raster angles significantly affect PLA material tensile properties. UV curing increased fragility and decreased stretch ability, while varying effects on tensile strength and modulus were observed. These findings will aid researchers in achieving sustainability in PLA materials and FDM technology.

Shergill et al. [14] used fused filament fabrication (FFF) to examine how the thickness of individual layers affects the mechanical characteristics of PLA and ABS samples created on a 3D printer. The results reveal that the mechanical qualities decline with increasing layer thickness; this is especially true for PLA's ultimate tensile strength. The research indicates that mechanical qualities, printing time, and simplicity should all be taken into account when determining the best print settings.

Shah and Jain [15] used two materials, Poly (lactic acid) (PLA) and carbon fiber-reinforced PLA (CF + PLA). The incorporation of CF reinforcement leads to increased Young's modulus and decreased tensile strength. The printing process induces microstructural alterations, with pronounced fiber breakage and misalignment. The strength of the printed part depends on the orientation, and both filament and printed parts exhibit intricate failure patterns. X-ray diffraction analysis reveals distinct variations in amorphous characteristics between the filament and printed component.

A multitude of studies have been conducted to examine the influence of the vascular system on the process of crack sealing in cementitious materials, as well as the utilization of recycled materials in concrete. These investigations encompass the following:

Created by Li et al. [16], a unique vascular network that has been inspired by the nature. It was created using law of Murray for the circulatory blood volume transfer. After sample has been broken up as well as pumped with the sodium silicate for 4 weeks, load recovery was utilized to restore its mechanical properties. The network's ability was to distribute and release the healing agent at the damage site, along with the system's compatibility with the surrounding matrix.

Li et al. [17] utilized 3D printing technology to fabricate a complex 3D internal hollow tunnel, using SEM and XRD techniques. Results showed calcite formation as the primary outcome of PVA-cement interaction.

De Nardi et al. [18] utilized tetrahedral mini-vascular networks (MVNs) made of PLA material by FDM, which were filled with sodium silicate and incorporated into cementitious matrices. Concrete beams have the capability to achieve strength recoveries of 20% and stiffness recoveries ranging from 75% to 80%.

Shields et al. [19] presented that glass tubes were attached to silicone tubes to ease the pumping of the healing agent. Examining a re-gain in the durability and mechanical qualities will help determine the healing agents' applicability in a self-healing vascular network system, together with polyurethanes, sodium silicate, and epoxy resin. Above 100% sealing efficiencies were attained, and the epoxy resin had a high strength regain.

Jongvivatsakul et al. [20] examined "model" material system, consisting of concrete structural parts with cyanoacrylate (CA) filled channels constructed of polyethelene terephthalate. The study's main emphasis was on the healing agent's transport and healing properties and their outcomes. The experimental program included the sorption of a healing agent via a broken surface into a concrete specimen and the capillary flow behavior of CA in a static natural crack.

Abdul Hamead et al. [21] described producing nano-powder as a weight percentage replacement of Portland cement for supporting mortar structural properties through XRD, SEM, and compression strength improvement. These improvements made the material useful for restoration and construction projects.

3D printing produces functional components with intricate geometries; examining mechanical performance and manufacturing parameters is crucial for design vascular tubes. For introducing autonomous self-healing characteristics as well as addressing the sensitivity regarding such materials to the formation of crack, multi-component inorganic sodium silicate was chosen as liquid with one nano-powder mineral (Fly Ash). This was done in order to establish a relation between the manufacturing parameters and mechanical properties of PLA pieces manufactured utilizing FDM carrying the various healing agents.

2. EXPERIMENTAL PART

The experimental work contains the following four parts:

(1) In order to conduct a parametric analysis on the

mechanical properties and identify the optimal selection of process parameters, the initial section of the study presents the prepared specimen, which is utilized to examine the properties under different layer thicknesses. The selection of a vascular network is made in order to design a system that can effectively deliver the healing agent to concrete.

(2) The vascular network system and samples were fabricated using a Creality CR-10S 3-D printer of Chinese origin, as depicted in Figure 1. This printer has a maximum printing dimension of 300 mm×300 mm×400 mm. The built orientations were evaluated to ensure they were upright. The printing parameters included a nozzle diameter of 0.8 mm, a platform temperature of 215℃, a 100% infill density, and a printing speed of 50 mm/s. The printing parameters for the filaments used in the preparation of fused deposition modeling (FDM) samples are presented in Table 1.

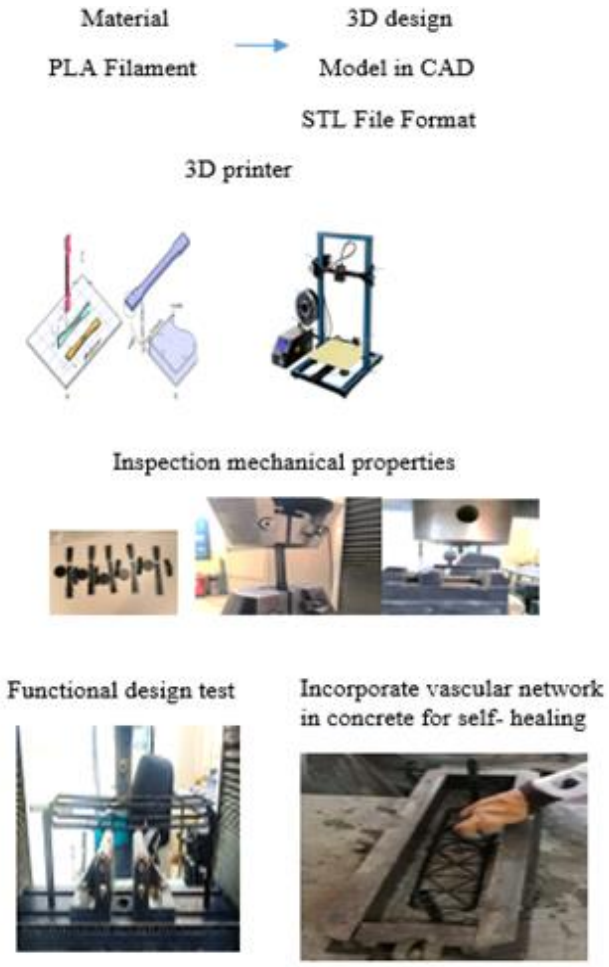

Figure 1. Design of a 1D, 2D and 3D Vascular network for self-healing in concrete beam

Based on the guidelines set forth by the ASTM standards, the process of generating three-dimensional (3D) models involves the utilization of computer-aided design (CAD) software, which subsequently converts these models into stereo lithography (STL) files, thereby facilitating the creation of test specimens. A diverse range of materials is commercially available in the form of filament spools for fused deposition modeling (FDM). Several factors need to be considered when utilizing materials as autonomous self-healing agents, such as their glass transition temperature (Tg), melting temperature (Tm), chemical resistance to coating and healing substances, and ability to withstand alkaline atmospheres in concrete. The glass transition temperature (Tg) of the selected material is a critical factor as it needs to demonstrate a relatively brittle behavior, characterized by higher tensile strength and lower elongation at rupture. This behavior is necessary to facilitate the release of the encapsulated healing ingredient. In conclusion, the utilization of inexpensive materials is favored in order to establish a self-healing system that is economically efficient. Poly lactic acid (PLA) is an aliphatic polyester that possesses bio-degradable properties. It is derived from sustainable sources such as sugarcane or corn. Polylactic acid (PLA) exhibits a lower glass transition temperature (Tg) of approximately 60℃ and demonstrates limited elongation at break, measuring less than 10% [22].

Printer parameters such as layer height, infill density, printing speed, nozzle temperature, and material choice influence the mechanical properties of printed objects [23]:

i. Layer thickness (mm) determines building part accuracy, with lower thickness affecting part accuracy, directly related to nozzle diameter
ii. Higher infill densities provide more material support, increasing mechanical strength.
iii. Slower printing speeds promote better heat dissipation and stronger interlayer adhesion.
iv. Nozzle temperature affects material flow and bonding between layers.
v. A 45/-45 raster angle enhances 3D printing mechanical properties by creating a crosshatch pattern, reducing anisotropy, and improving layer adhesion, resulting in stronger, stiffer, and better-quality objects.
vi. Material choice directly impacts mechanical properties.

Finding the optimal combination of parameters requires experimentation and testing.

(3) In this study, the production of nano-powder derived from fly ash was conducted through the utilization of a planetary ball mill equipped with ceramic balls. The milling process was carried out at a rotational speed of 400 revolutions per minute (rpm) for a duration of three hours. Subsequently, the resulting nano-powder was blended with sodium silicate solution at concentrations of 5%, 10%, and 15% to serve as a healing material. The objective of this investigation was to assess the compatibility of these materials with the poly (lactic acid) (PLA) tube embedded within concrete.

Table 1. Printing parameters for PLA material configurations

Printing Parameters	Configurations
Height of each layer (mm)	0.1, 0.2, 0.3, 0.4, 0.5
Layer orientation	Up right
Optimal temperature for printing	215 (℃)
Bed temperature (℃)	60
Diameter of filament (mm)	1.75
Diameter of nozzle (mm)	0.8
Speed of printing (mm/s)	50 mm/s
Raster angle	45/-45
Travel speed (mm/s)	150 mm/s
In fill	100%

2.1 Software used

Max test software for tensile and flexural test. Computer-aided design (CAD) software Next, establish a connection between the design file and the stereo lithography (STL) of the 3D printing equipment to transfer the required geometric information for producing the tubes.

3. INSPECTION

3.1 The inspections of nano-powder

The assessment of the particle size of fly ash powder was conducted at the Nanotechnology and Advanced Research Center using the Brookhaven Nano Brook 90 plus US instrument. It was discovered 100 nm.

3.2 Mechanical properties

3.2.1 Tensile test

Tensile test was achieved in accordance with the ASTM standard (D638-10) using a universal tensile instrument of type (WDW-50) made by the Lariee Company in China, at a (5 mm/min) cross-head speed and a force of 5 KN until the specimen breaks. Tensile characteristics, including elastic modulus, tensile strength, and elongation (%) at break were obtained by the tensile test [24]. Figure 2(a) views the used tensile strength instrument and Figure 2(b) illustrates the image of specimens after the test.

(a) Tensile strength instrument

(b) The image of specimens after test

(c) Flexural strength instrument

Figure 2. Inspection mechanical properties

3.2.2 Flexural test

The three-point flexural test was conducted using the three-point bending test technique at the same universal test instrument (Figure 2(c)) that was utilized for the tensile test. To get the load-displacement curve, which depicts the relation between displacement (mm) and force (N) for all the prepared specimens, the vertical force was applied at the center of the composite specimens using this approach. For each composite sample created in accordance with the ASTM standard (D790-10), the values acquired from this test are the flexural modulus and flexural strength. The formula below was used to calculate the test specimen's maximum flexural strength at any point along the load-extension curve [25]:

$$F.S = \frac{3pl}{2bh^2} \quad (1)$$

where,
$F.S$ = Bending strength (N/mm^2)
p = Fracture load (N)
l = Support span (mm)
b = A specimen's width (mm)
h = Thickness of specimen (mm)

3.2.3 Hardness test

A Shore-D hardness test was performed on specimens, and in order to obtain very accurate findings, an average of six readings had to be taken at various spots on each sample. According to ASTM standard (D2240) [26], the specimen should have a minimum diameter of 40 mm and a minimum thickness of 3 mm to pass the hardness test utilizing the Durometer hardness test. The applied load was 50 N, and the measuring dwell time was equal to (sec).

3.3 Physical properties

3.3.1 Determination of the water absorption of 3D-printed samples

The water absorption of samples was tested in accordance with ISO 62 [27]. After being immersed in distilled water for a period of time at the room temperature and being removed from the water afterward, five 3D-printed samples were weighed in a scale with a (0.0001 g) precision after absorbing any remaining water on surface using an absorbent, lint-free cloth. All the samples were then immersed once more in distilled water. Eq. (2) was employed to calculate the (%) of gain X_t at the time (t) due to the water uptake. Until the sample mass was nearly consistent, this was repeated.

$$Xt = \frac{Wt - Wo}{Wo} \times 100\% \quad (2)$$

where, W_t and W_0 represent the weight of the sample after and before exposing to the water, respectively.

4. RESULTS AND DISCUSSION

4.1 Particle size distribution (PSD) results

The Fly Ash nanoparticles resulting from the ball milling process were analyzed using a PSA instrument to determine the particle size and size distribution during the milling

technique. Following the PSA, the particle size of the Fly Ash was effectively reduced to 95.3 nm after milling for a duration of 3 hours. Figure 3 shows the particle size distribution of the nano-powder that was manufactured.

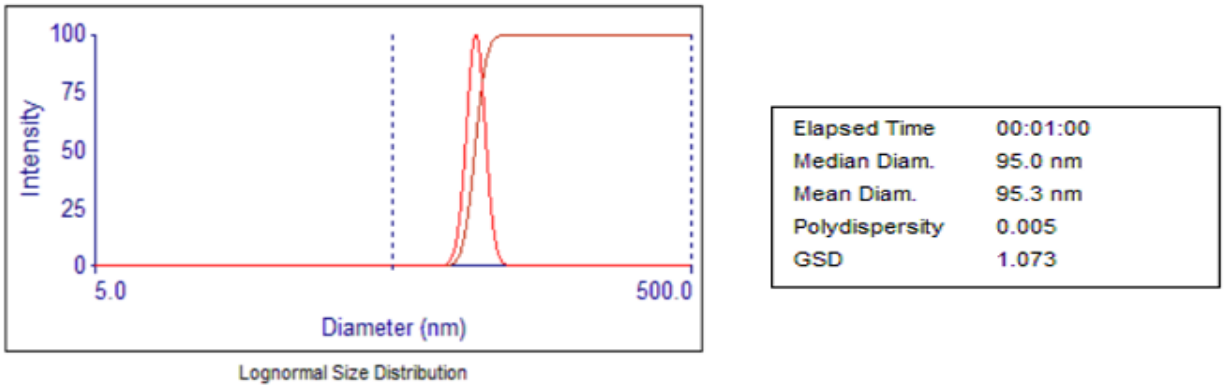

Figure 3. Characterization of the particle size distribution of the produced nano-powder

4.2 Tensile test results

The number of layers necessary for the printing of an object is directly correlated with the thickness of each individual layer. Figure 4 illustrates various process variables, including the average maximum tensile strength as a function of layer thickness. The mechanical properties are influenced by the layer thickness due to the construction orientation. In instances where the samples were positioned vertically, it was observed that an increase in layer thickness corresponded to an enhancement in strength. The results of this study were in line with the previous research conducted [28]. This phenomenon can be rationalized by postulating that an increase in the thickness of the layer leads to in a reduced number of layers necessary to achieve a specific total thickness. Consequently, this reduction in layer count leads to a decrease in the number of layer bonds, thereby enhancing the overall strength. The results demonstrated that there was an increase in both flexural and tensile strength as the layer thickness increased in the case of the upright orientation. These variations can be elucidated by two main failure modes: inter-layer fusion bond failure (referred to as inter-layer failure) and trans-layer failure. The failure of the inter-layer fusion link in the upright orientation can be attributed to the perpendicular pulling of the samples in relation to the direction of layer deposition, with the force being parallel to their respective layers (see Figure 4). The primary load in this case was borne by the inter-layer fusion bonds between adjacent layers, rather than by the individual layers themselves. The tensile strength was significantly influenced by the adhesion between layers. The anticipated tensile strength was found to be lower than that of the individual layers [29, 30]. The addition of 0.5 mm to the thickness of the layer resulted in the creation of bigger spaces, therefore causing an increase in the porosity inside the specimen's cross section. The existence of higher porosity resulted in reduced mechanical characteristics [29].

4.3 Flexural strength test results

Figure 5 illustrates the relationship between layer thickness and the average maximum flexural strengths and modulus elasticity. The thickness of each sample layer ranges from 0.1 mm to 0.5 mm, with a uniform thickness of 4 mm for each sample. The flexural strength measurement varies due to the variability in the maximum load capacity of each specimen. In this particular case, it is generally observed that an increased thickness of the layer tends to promote a stronger adhesive bond. The observed results were in accordance with the previous research conducted on PLA [4, 31]. Thicker layers appeared to promote increased strength. The tensile strength of the layer increases proportionally with its thickness, resulting in a stronger bond capable of withstanding bending loads. The findings demonstrated that the upright orientation generally exhibited brittle behavior. However, at a thickness of 0.5 mm, the opposite phenomenon was observed.

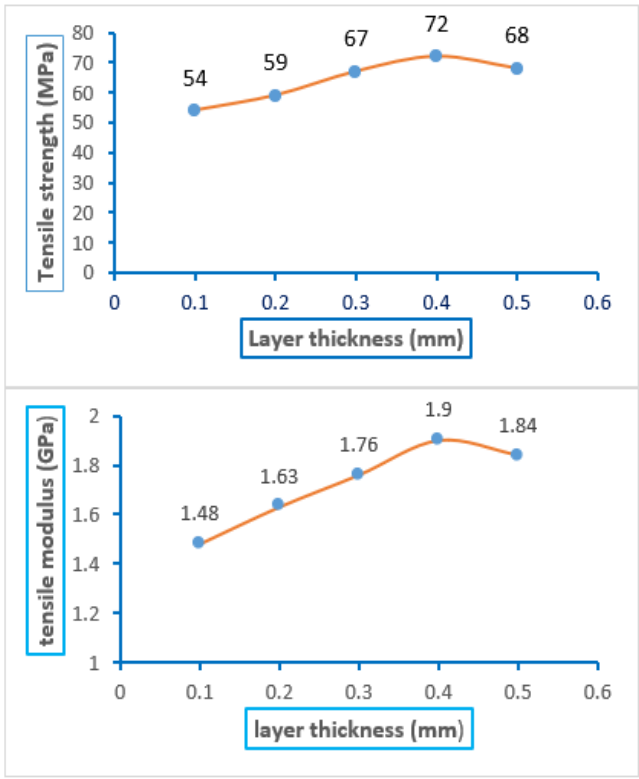

Figure 4. Tensile strength and tensile modulus varying with the layer thickness results

4.4 Hardness test results

The mechanical properties of the filaments, the bonding forces between the filaments in same layer, and the bonding forces between layers are three crucial factors that influence the hardness properties of polylactic acid (PLA) samples with

a 100% infill density. The augmentation of inter-filament adhesion within a given layer is a direct consequence of elevating the density of infill. The application of a 100% infill density results in an increase in the hardness of the specimens, as a greater amount of material is present to withstand external forces. According to a study conducted by researchers [32], it has been observed that there is a slight reduction in the hardness of the material as the thickness of the layer increases. Figure 6 provides a clear illustration of the relationship between the hardness, measured in Shore-D units, and the thickness of the layers.

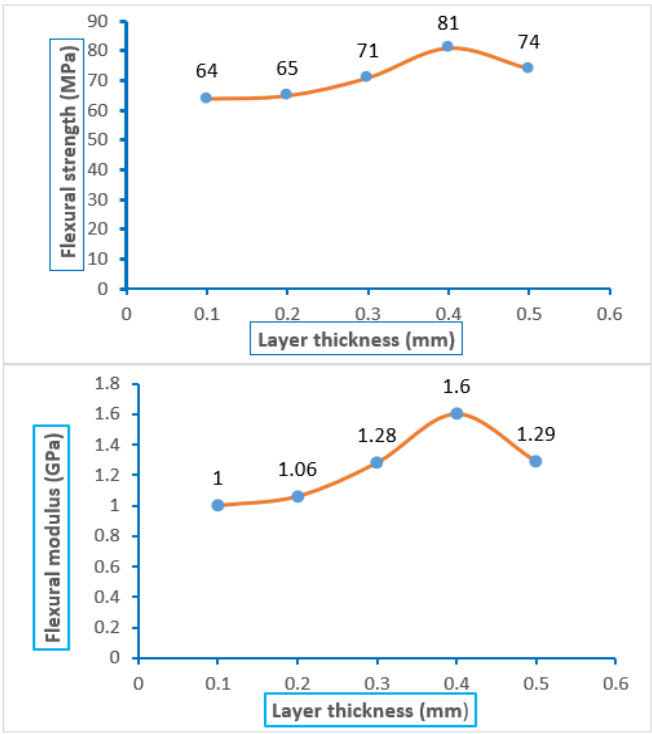

Figure 5. Flexural strength and flexural modulus varying with the layer thickness results

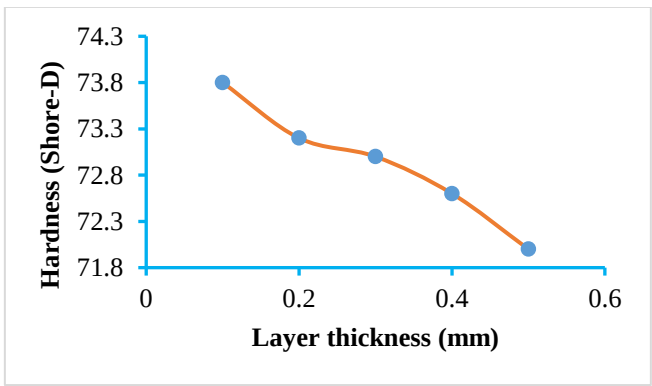

Figure 6. Hardness (Shore-D) varying with the layer thickness results

4.5 Water resistance results

Water resistance of the PLA specimens manufactured in 3D was tested. The samples densities ranged from 0.87 to 1.00 g/cm^3. Beyond 4 weeks of immersion in water at a natural temperature and an increase in the printing layer thickness from 0.1 mm to 0.5 mm, the samples water absorption did not alter noticeably. This could be explained by the samples lack of porosity as the thickness of printing layer increased, which prevented any water absorption. In the case when a single layer remains in a molten condition and is bounded to a solid layer whilst solidifying, a bonding between the layers will be produced as a result of the interaction of molecules, and better bonding when the temperature is sufficient to increase the adhesion between the layers and prevent the formation of gaps between the layers [8, 33].

4.6 Functional design test results

The study aimed to demonstrate the feasibility of implementing previously discovered principles by undertaking the design and production of a vascular network for self-healing within a concrete beam. In order to evaluate the functional structural strength, the researchers conducted bending tests and considered the maximum load at failure as the basis for comparing strengths. The selection process involved choosing combinations of the upright and layer thickness, as well as determining the average and standard deviation of the failure maximum load. In a broad sense, it can be observed that the bending performance of the design aligns with the findings of the coupons and demonstrates the fundamental patterns observed in the upright samples, where an increase in layer thickness corresponds to an increase in strength. The samples that were oriented in an upright position exhibited a brittle fracture behavior. Consequently, the interplay between the thickness of the layers, the orientation of the construction, and the rate at which material is fed had a notable impact on the maximum strength (Fmax) of the functional structure. This was observed through variations in the average values across different sets of process parameters, falling within the range of 25-75 N. The hollow vascular network system was fabricated using three-dimensional printing technology, employing a 3D modeling network. The dimensions of the printed network were then compared to those of the corresponding one-dimensional (1D) and two-dimensional (2D) networks, both having an outer diameter of 5.6 mm and an inner diameter of 4 mm. The study involves incorporating a combination of healing agents into a liquid solution of inorganic sodium silicate. This solution is then mixed with a nano-powder mineral called Fly Ash and applied to concrete beams. The aim is to introduce self-healing properties to the concrete and address its susceptibility to crack formation. Figure 7 illustrates the three-dimensional printed vascular network composed of polylactic acid (PLA) with various design configurations.

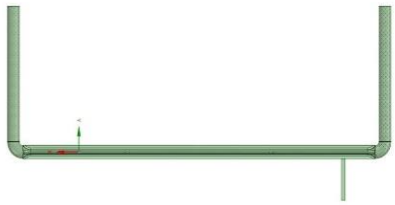

(a) One dimension

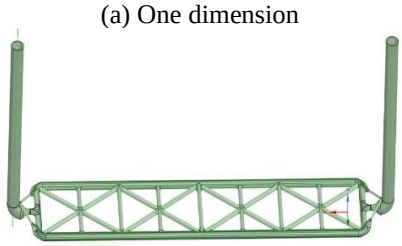

(b) Two dimensions

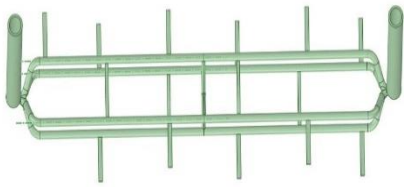

(c) Three dimensions

Figure 7. 3D printed vascular network from PLA with different designs

5. CONCLUSIONS, LIMITATION AND FUTURE PERSPECTIVES

5.1 Conclusions

In the present work, the researchers investigated the impact of the layer thicknesses are 0.1, 0.2, 0.3, 0.4, and 0.5 mm, built orientation (Upright), and feed rate (Fr = 40 mm/s) on the mechanical characteristics of polylactic acid (PLA) samples made with a three-dimensional printer. Following the guidelines of ASTM standard, tensile and A series of 3-point bending tests were performed to determine the mechanical behavior of the printed samples. In the case when the functional part is printed in an upright orientation, the goal of the investigation is to choose the particular parameters that will allow for the creation of a hollow network of tubes imbedded inside the concrete for self-healing.

The observed decrease in ductility can be attributed to the increase in layer thickness and feed rate. Nevertheless, it was observed that the mechanical properties exhibited an upward trend as the layer thickness increased up to a specific point. Specifically, the flexural strength showed an increase to 81 MPa, while the flexural modulus also experienced an enhancement to 1.6 GPa. Using higher infill densities provides more material support throughout the printed object, leading to improved tensile strength to 72 MPa and tensile modulus to 1.9 GPa at Lt = 0.4 mm. The hydrophobic properties of the material have been demonstrated through a water absorption test.

Depending on the construction orientation, infill density 100% and 45/-45 raster angel, the layer thickness had a distinct impact on the flexural and tensile strength related to PLA samples. Greater gaps resulted from the layer thickness increase up to 0.5 mm, which raised the porosity in the specimen's cross section. Lower mechanical properties were the result of greater porosity.

5.2 Limitation

(1) Small sample size.

(2) Single material used: The focus on PLA as both the printing material and healing agent disregarded the potential effects of different materials or material combinations on the mechanical properties.

(3) Short-term assessment: The study evaluated the compatibility of materials with the PLA tube inside concrete for a short duration, leaving out a comprehensive assessment of long-term durability and performance.

(4) Limited generalizability: The findings may specifically apply to the materials, printer, and experimental setup employed in this study, and their relevance to other scenarios may vary. Additional research and experimentation are needed for broader generalization.

5.3 Future perspectives

Future work should focus on integrating advanced sensors for real-time monitoring, optimizing influential vascular healing networks, developing improved healing agents, conducting performance evaluations, implementing self-healing concrete in field projects, and assessing sustainability aspects for more resilient and durable infrastructure.

REFERENCES

[1] Cuan-Urquizo, E., Barocio, E., Tejada-Ortigoza, V., Pipes, R.B., Rodriguez, C.A., Roman-Flores, A. (2019). Characterization of the mechanical properties of FFF structures and materials: A review on the experimental, computational and theoretical approaches. Materials, 12(6): 895. https://doi.org/10.3390/ma12060895

[2] Lupone, F., Padovano, E., Veca, A., Franceschetti, L., Badini, C. (2020). Innovative processing route combining fused deposition modelling and laser writing for the manufacturing of multifunctional polyamide/carbon fiber composites. Materials & Design, 193: 108869. https://doi.org/10.1016/j.matdes.2020.108869

[3] Vu, M.C., Jeong, T.H., Kim, J.B., Choi, W.K., Kim, D.H., Kim, S.R. (2021). 3D printing of copper particles and poly (methyl methacrylate) beads containing poly (lactic acid) composites for enhancing thermomechanical properties. Journal of Applied Polymer Science, 138(5): 49776. https://doi.org/10.1002/app.49776

[4] Chacón, J.M., Caminero, M.A., García-Plaza, E., Núnez, P.J. (2017). Additive manufacturing of PLA structures using fused deposition modelling: Effect of process parameters on mechanical properties and their optimal selection. Materials & Design, 124: 143-157. https://doi.org/10.1016/j.matdes.2017.03.065

[5] Liu, X., Zhang, M., Li, S., Si, L., Peng, J., Hu, Y. (2017). Mechanical property parametric appraisal of fused deposition modeling parts based on the gray Taguchi method. The International Journal of Advanced Manufacturing Technology, 89: 2387-2397. https://doi.org/10.1007/s00170-016-9263-3

[6] Aveen, K.P., Bhajathari, F.V., Jambagi, S.C. (2018). 3D printing & mechanical characteristion of polylactic acid and bronze filled polylactic acid components. IOP Conference Series: Materials Science and Engineering, 012042. https://doi.org/10.1088/1757-899X/376/1/012042

[7] Vinyas, M., Athul, S.J., Harursampath, D. (2019). Mechanical characterization of the Poly lactic acid (PLA) composites prepared through the Fused Deposition Modelling process. Materials Research Express, 6(10): 105359. https://doi.org/10.1088/2053-1591/ab3ff3

[8] Ayrilmis, N., Kariz, M., Kwon, J.H., Kitek Kuzman, M. (2019). Effect of printing layer thickness on water absorption and mechanical properties of 3D-printed wood/PLA composite materials. The International Journal of Advanced Manufacturing Technology, 102: 2195-2200. https://doi.org/10.1007/s00170-019-03299-9

[9] Nabipour, M., Akhoundi, B. (2021). An experimental

study of FDM parameters effects on tensile strength, density, and production time of ABS/Cu composites. Journal of Elastomers & Plastics, 53(2): 146-164. https://doi.org/10.1177/0095244320916838

[10] Ali, H.B., Oleiwi, J.K., Othman, F.M. (2022). Compressive and tensile properties of ABS material as a function of 3D printing process parameters. Revue des Composites et des Matériaux Avancés-Journal of Composite and Advanced Materials, 32(3): 117-123. https://doi.org/10.18280/rcma.320302

[11] Triyono, J., Sukanto, H., Saputra, R.M. Smaradhana, D.F. (2020). The effect of nozzle hole diameter of 3D printing on porosity and tensile strength parts using polylactic acid material. Open Engineering, 10(1): 762-768. https://doi.org/10.1515/eng-2020-0083

[12] Bakır, A.A., Atik, R., Özerinç, S. (2021). Effect of fused deposition modeling process parameters on the mechanical properties of recycled polyethylene terephthalate parts. Journal of Applied Polymer Science, 138(3): 49709. https://doi.org/10.1002/app.49709

[13] Hsueh, M.H., Lai, C.J., Chung, C.F., Wang, S.H., Huang, W.C., Pan, C.Y., Zeng, Y.S., Hsieh, C.H. (2021). Effect of printing parameters on the tensile properties of 3D-printed polylactic acid (PLA) based on fused deposition modeling. Polymers, 13(14): 2387. https://doi.org/10.3390/polym13142387

[14] Shergill, K., Chen, Y., Bull, S. (2023). An investigation into the layer thickness effect on the mechanical properties of additively manufactured polymers: PLA and ABS. The International Journal of Advanced Manufacturing Technology, 126(7-8): 3651-3665. https://doi.org/10.1007/s00170-023-11270-y

[15] Shah, A.K., Jain, A. (2023). Microstructure and mechanical properties of filament and fused deposition modelling printed polylactic-acid and carbon-fiber reinforced polylactic-acid. Journal of Reinforced Plastics and Composites. https://doi.org/10.1177/07316844231167551

[16] Li, Z., de Souza, L.R., Litina, C., Markaki, A.E., Al-Tabbaa, A. (2020). A novel biomimetic design of a 3D vascular structure for self-healing in cementitious materials using Murray's law. Materials & Design, 190: 108572. https://doi.org/10.1016/j.matdes.2020.108572

[17] Li, Z., Souza, L.R.D., Litina, C., Markaki, A.E., Al-Tabbaa, A. (2019). Feasibility of using 3D printed polyvinyl alcohol (PVA) for creating self-healing vascular tunnels in cement system. Materials, 12(23): 3872. https://doi.org/10.3390/ma12233872

[18] De Nardi, C., Gardner, D., Jefferson, A.D. (2020). Development of 3D printed networks in self-healing concrete. Materials, 13(6): 1328. https://doi.org/10.3390/ma13061328

[19] Shields, Y., Van Mullem, T., De Belie, N., Van Tittelboom, K. (2021). An investigation of suitable healing agents for vascular-based self-healing in cementitious materials. Sustainability, 13(23): 12948. https://doi.org/10.3390/su132312948

[20] Jongvivatsakul, P., Ramdit, T., Ngo, T.P., Likitlersuang, S. (2018). Experimental investigation on mechanical properties of geosynthetic cementitious composite mat (GCCM). Construction and Building Materials, 166: 956-965. https://doi.org/10.1016/j.conbuildmat.2018.01.185

[21] Abdul-Hamead, A.A., Othman, F.M., Hmeed, N.A. (2018). The effect of nano fly ash on properties of cement mortar. In 4th Electronic and Green Materials International Conference 2018 (EGM 2018), Bandung, Indonesia, p. 020011. https://doi.org/10.1063/1.5080824

[22] Kumar, N., Kumar Jain, P. (2021). Analysing the influence of raster angle, layer thickness and infill rate on the compressive behaviour of EVA through CNC-assisted fused layer modelling process. In Proceedings of the Institution of Mechanical Engineers, Part C: Journal of Mechanical Engineering Science, 235(10): 1731-1740. https://doi.org/10.1177/0954406219889076

[23] Anglani, G.I., Antonaci, P.A., Gonzales, S.I., Paganelli, G.I., Tulliani, J.M. (2019). 3D printed capsules for self-healing concrete applications. In Proceedings of the 10th International Conference on Fracture Mechanics of Concrete and Concrete Structures (FraMCoS-X), Bayonne, France, pp. 24-26. https://doi.org/10.21012/FC10.235356

[24] ASTM, S. (2010). Test method for tensile properties of plastics. In Annual Book of ASTM Standards D638. American Society for Testing and Materials, West Conshohocken, PA, USA.

[25] ASTM, S. (2010). Test method for flexural properties of unreinforced and reinforced plastics and electrical insulating materials. In Annual book of ASTM standards D790. American Society for Testing and Materials, West Conshohocken, PA, USA.

[26] ASTM, S. (2003). Standard Test Method for Rubber Property—Durometer Hardness. Annual book of ASTM standards D2240-03. In American Society for Testing and Materials, West Conshohocken, PA, USA.

[27] ISO, S. (2008). Plastics - determination of water absorption. ISO62. International Organization for Standardization, Geneva.

[28] Sood, A.K., Ohdar, R.K., Mahapatra, S.S. (2010). Parametric appraisal of mechanical property of fused deposition modelling processed parts. Materials & Design, 31(1): 287-295. https://doi.org/10.1016/j.matdes.2009.06.016

[29] Domingo-Espin, M., Puigoriol-Forcada, J.M., Garcia-Granada, A.A., Llumà, J., Borros, S., Reyes, G. (2015). Mechanical property characterization and simulation of fused deposition modeling Polycarbonate parts. Materials & Design, 83: 670-677. https://doi.org/10.1016/j.matdes.2015.06.074

[30] Lanzotti, A., Grasso, M., Staiano, G., Martorelli, M. (2015). The impact of process parameters on mechanical properties of parts fabricated in PLA with an open-source 3-D printer. Rapid Prototyping Journal, 21(5): 604-617. https://doi.org/10.1108/RPJ-09-2014-0135

[31] Wang, X., Jiang, M., Zhou, Z., Gou, J., Hui, D. (2017). 3D printing of polymer matrix composites: A review and prospective. Composites Part B: Engineering, 110: 442-458. https://doi.org/10.1016/j.compositesb.2016.11.034

[32] Rodríguez-Panes, A., Claver, J., Camacho, A.M. (2018). The influence of manufacturing parameters on the mechanical behaviour of PLA and ABS pieces manufactured by FDM: A comparative analysis. Materials, 11(8): 1333. https://doi.org/10.3390/ma11081333

[33] Patil, A.Y., Banapurmath, N.R., EP, S., Chitawadagi, M.V., Khan, T.Y., Badruddin, I.A., Kamangar, S. (2020). Multi-scale study on mechanical property and strength of new green sand (Poly Lactic Acid) as replacement of fine

aggregate in concrete mix. Symmetry, 12(11): 1823. https://doi.org/10.3390/sym12111823

NOMENCLATURE

FDM	Fused Deposition Modeling
PLA	Polylactic Acid
AM	Additive Manufacturing
PETG	Polyethylene Terephthalate Glycol
ABS	Acrylonitrile Butadiene Styrene
PC	Polycarbonate
FFF	Fused Filament Fabrication
SEM	Scanning Electron Microscope
XRD	X-Ray Diffraction Analysis
STL	Stereo Lithography
g	gram
RPM	Revolutions Per Minute
Sec	Second